Germline and Somatic *DICER1* Mutations in a Pituitary Blastoma Causing Infantile-Onset Cushing's Disease

Taninee Sahakitrungruang, Chalurmpon Srichomthong, Sopon Pornkunwilai, Jiraporn Amornfa, Shanop Shuangshoti, Supasak Kulawonganunchai, Kanya Suphapeetiporn, and Vorasuk Shotelersuk

Division of Pediatric Endocrinology (T.S., S.P.), Center of Excellence for Medical Genetics, Department of Pediatrics (C.S., S.K., K.S., V.S.), Division of Neurosurgery, Departments of Surgery (J.A.) and Pathology (S.S.), Faculty of Medicine, Chulalongkorn University; and Excellence Center for Medical Genetics (C.S., S.K., K.S., V.S.), King Chulalongkorn Memorial Hospital, Thai Red Cross Society, Bangkok 10330, Thailand

Context: Pituitary blastoma causing Cushing's syndrome in infancy is very rare, and its molecular pathomechanism is not well understood.

Objective: Our objective was to identify genetic changes of a pituitary blastoma causing infantile-onset Cushing's syndrome in a Thai girl without a family history of cancers.

Methods: Genomic DNA from both leukocytes and tumor tissues was used for whole-exome sequencing (WES) and Sanger sequencing of *DICER1*. The cDNA reverse-transcribed from RNA extracted from both leukocytes and tumor tissues was used for Sanger sequencing, quantitative real-time PCR (qRT-PCR), and pyrosequencing of *DICER1*.

Results: WES of leukocytes identified a novel heterozygous c.3046delA (p.S1016VfsX1065) mutation in the *DICER1* gene. WES of the tumor tissues detected the same frameshift germline mutation and another novel somatic missense c.5438A→T (p.E1813V) mutation. Both mutations were validated by Sanger sequencing. Quantitative real-time PCR revealed that the *DICER1* mRNA levels of the tumor tissues were 54% compared with those of her leukocytes. Pyrosequencing showed that the deletion allele constituted 12% and 0% of the *DICER1* cDNA of the proband's leukocytes and tumor tissues, respectively.

Conclusion: Our study extends the phenotypic and mutational spectrum of *DICER1* mutations to include infantile-onset Cushing's disease and 2 novel mutations. Loss of function of both *DICER1* alleles appears to be crucial to initiate tumor development. **(*J Clin Endocrinol Metab* 99: E1487–E1492, 2014)**

An ACTH-producing pituitary tumor or Cushing's disease is unusual in infants (1–12). The first case reported in 1979 described a large, histologically unique pituitary tumor that was unrelated to Cushing's microadenomas in older children or adults (1). Subsequently, a few more similar cases of infantile-onset Cushing's disease were reported (2, 4, 7). The histopathology of these tumors appears to be consistent with pituitary blastoma, a term later coined in 2008 (10, 11).

The *DICER1* gene encodes an endoribonuclease responsible for processing hairpin precursor microRNAs (miRNAs) into functional miRNAs. In 2007, *DICER1* was first identified as an oncogene in pulmonary adenomas (13). Subsequently, it was found to be associated with pleuropulmonary blastoma (14) and was later recognized as the basis of a pleiotropic tumor syndrome (15). In 2011, an infant with pituitary blastoma was reported to have a germline heterozygous *DICER1*

ISSN Print 0021-972X ISSN Online 1945-7197
Printed in U.S.A.

Received January 2, 2014. Accepted May 2, 2014.
First Published Online May 13, 2014

Abbreviations: gDNA, genomic DNA; HDDST, high-dose dexamethasone suppression test; miRNA, microRNA; RNase, ribonuclease; WES, whole-exome sequencing.

mutation (12), but the full description was not published.

Here, we describe a Thai infant with Cushing's syndrome caused by an aggressive pituitary blastoma. Whole-exome sequencing (WES) of both leukocytes and tumor tissues identified 2 novel mutations in *DICER1*. For the first time, genomic DNA (gDNA) and RNA of the tumor tissues were studied.

A 12-month-old female Thai infant presented with an increased appetite 1 month and right ophthalmoplegia and ptosis 1 week before an initial visit. History of consanguinity and cancers in family members were denied. On examination, she was a chubby infant with a Cushingoid appearance including a round face, buffalo hump, and hirsutism. Striae and acne were absent. Her weight and length were 10 kg (+1.0 SD) and 78 cm (+1.0 SD), respectively. She followed normal growth curves. Her blood pressure was 106/63 mm Hg (+1.1/+0.9 SD).

Biochemical evaluation revealed the following: hemoglobin, 13.8 g/dL; blood urea nitrogen, 11 mg/dL; creatinine, 0.23 mg/dL; Na, 141 mmol/L; K, 3.8 mmol/L; Cl, 104 mmol/L; HCO_3, 22 mmol/L; and blood glucose, 101 mg/dL. Her bone age was 1 year and 6 months. Endocrine studies showed raised midnight cortisol levels at 46 μg/dL and elevated ACTH at 139 pg/mL. A low-dose dexamethasone suppression test failed to suppress serum cortisol (22.8 μg/dL) and ACTH (191 pg/mL). A single high-dose dexamethasone suppression test (HDDST) showed nonsuppressible morning cortisol (91 μg/dL) and ACTH (190 pg/mL). Other hormonal studies were normal including the following: free T_4, 1.33 ng/dL; TSH, 0.458 μU/mL; prolactin, 0.9 ng/mL; IGF-1, 127 ng/ml; IGF binding protein 3, 2500 μg/L; β-human chorionic gonadotropin, <5 mU/mL; and alpha-fetoprotein, 48.46 IU/mL.

MRI of the brain showed a $2.9 \times 2 \times 2.8$ cm heterogeneous enhancing lobulated mass in the sellar and suprasellar regions, with an involvement of the right cavernous sinus (Figure 1A). The lesion compressed the right optic nerve and encased the cavernous segment of the right internal carotid artery. Bifrontal craniotomy revealed a grayish brown tumor with contact bleeding. Partial resection (~30%) was achieved.

Histopathologically, epithelial cells with glandular formation were admixed with sheets and lobules of round tumor cells (Figure 1B). Mitotic figures were identified, 8 to 10 per 10 high-power fields. The epithelial component strongly expressed AE1/AE3 cytokeratin (Supplemental Figure 1A) and galectin-3. The round tumor cells were reactive with synaptophysin (Supplemental Figure 1B) and chromogranin. On adenohypophyseal hormonal stains, 40% and 20% of the round cells expressed ACTH and FSH, respectively (Supplemental Figure 1C). Ki-67 index was prominent in the epithelial part, up to 20%. These pathological features are diagnostic of pituitary blastoma.

Given the malignant histology, chemotherapy including cyclophosphamide, vincristine, methotrexate, carboplatin, and etoposide was given immediately after the surgery. Her morning cortisol declined to 25.9 and 21.0 μg/dL at 1 and 3 months after the surgery and chemotherapy, respectively. At a 4-month-follow up, she had stable right ophthalmoplegia and ptosis but was otherwise healthy. Her morning cortisol levels were 31 μg/dL, and ACTH was 122 pg/mL. Unfortunately, the patient died due to complications of the catheter-port operation for chemotherapy at the age of 1 year and 4 months.

Materials and Methods

Whole-exome sequencing

WES was performed using high-quality gDNA from either leukocytes or tumor tissues. The gDNA was sent to Macrogen Inc for next-generation sequencing. DNA was captured on the TruSeqExome Enrichment Kit (Illumina) and subsequently sequenced on the Hiseq2000 instrument. Sequence reads were mapped against UCSC hg19 using BWA software (http://bio-bwa.sourceforge.net/). The single-nucleotide polymorphisms (SNPs) and Indels were detected by SAMTOOLS (http://samtools.sourceforge.net/) and annotated by dbSNP&1000G. SNPs and indels were further filtered. After quality filtering, we looked for variants located in coding regions that were discordant between leukocytes and tumor tissues.

Sanger sequencing

The gDNA of both leukocytes and tumor tissues were PCR-amplified and Sanger-sequenced to confirm the presence of mutations identified by WES. The entire coding regions of *DICER1* cDNA were also sequenced. Primer pairs for amplification of exons 19 and 25 of *DICER1* gDNA and of the entire coding sequences of *DICER*1 cDNA are listed in Supplemental Table 1.

RNA analyses

Total RNA was isolated from leukocytes and tumor tissues using the QIAamp RNA Blood Mini kit (QIAGEN) and was reverse-transcribed to cDNA. The qRT-PCR to detect *DICER1* expression was performed by using SYBR Green on the cDNA of a control's leukocytes and the proband's leukocytes and tumor tissues. To explore a proportion of the expression levels of c.3046delA vs c.5438A→T mutations, pyrosequencing was used. Specific allele sequencing was performed by using PyroMark Q24 (QIAGEN). The primers are shown in Supplemental Table 2. All data were analyzed using PyroMark software with Aq mode. Experiments were performed 2 times in triplicate.

Results

Exome sequencing identified 112 402 variants in either leukocytes or tumor tissues. After quality filtering, 65 527 vari-

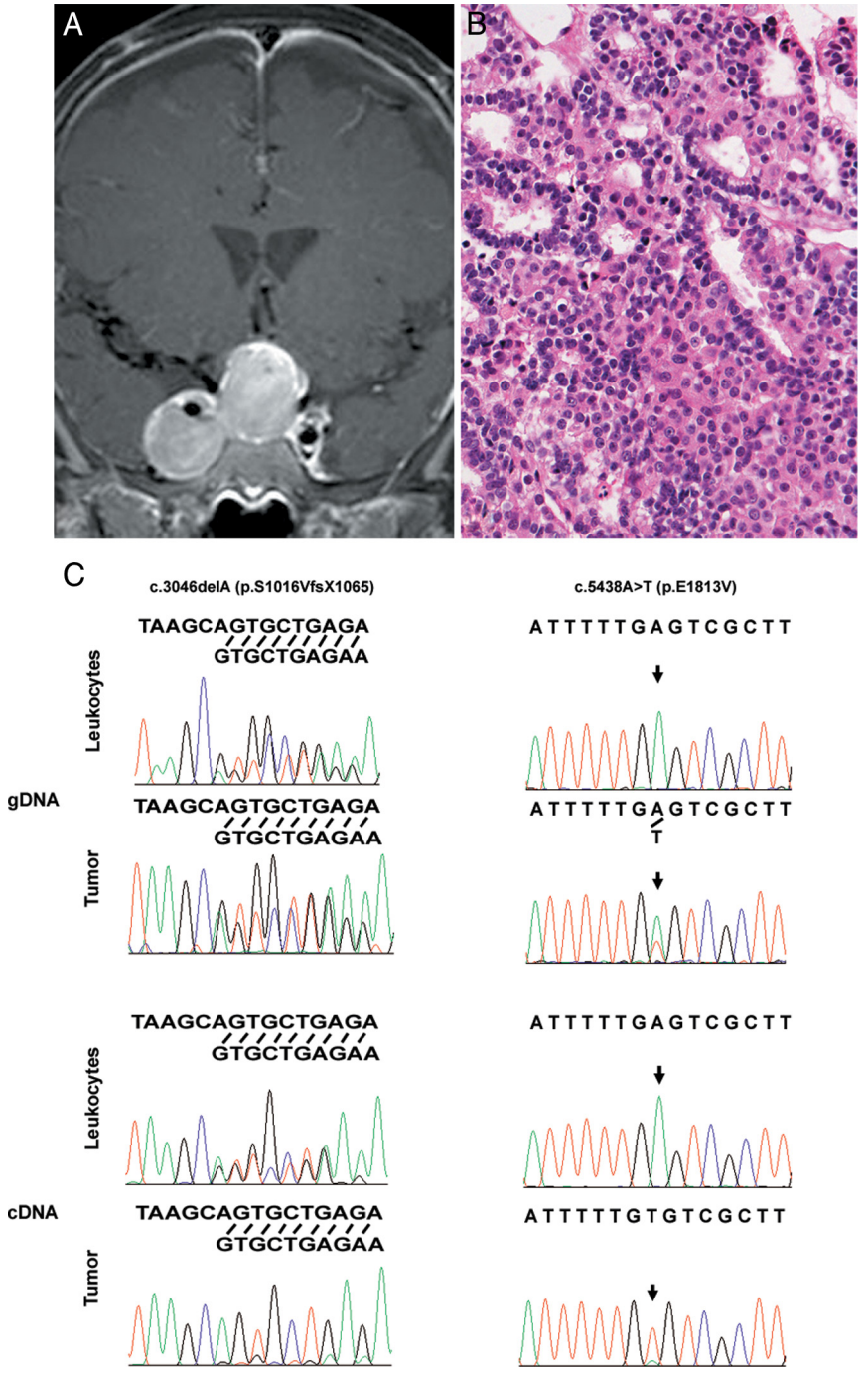

Figure 1. Brain MRI (A), histopathological features (B), and *DICER1* mutation analysis (C). A, a 2.9 × 2 × 2.8 cm heterogeneous enhancing lobulated mass in the sellar and suprasellar regions. B, Epithelial cells with glandular formation admixed with sheets and lobules of round tumor cells (hematoxylin and eosin; original magnification, ×400). C, Upper panel: electropherogram of the patient using gDNA as template reveals a heterozygous frameshift mutation c.3046delA (p.S1016VfsX1065) in both leukocytes and tumor tissues (left panel) and a heterozygous missense mutation c.A5438T (p.E1813V) only in tumor tissues (right panel, arrow); lower panel, electropherogram of the patient using cDNA as template shows a heterozygous frameshift mutation c.3046delA (p.S1016VfsX1065) in leukocytes. This mutation was almost undetectable in tumor tissues (left panel). The missense c.A5438T (p.E1813V) mutation was present only in tumor tissues with almost undetectable wild-type A allele at the 5438 position (right panel, arrow).

ants remained. Eight variants were different between leukocytes and tumor tissues. Only 1, c.A5438T (p.E1813V) in the *DICER1* gene was in the coding region. This missense mutation was present in a heterozygous state in tumor tissues, whereas leukocytes had only the wild-type allele, suggesting that it was a somatic mutation. Interestingly, no other coding variants different between leukocytes and tumor tissues were detected.

We then checked the remaining sequences of *DICER1* and found another heterozygous c.3046delA (p.S1016VfsX1065) in both leukocytes and tumor tissues, suggesting that this frameshift was a germline mutation. Sanger sequencing of the gDNA of both leukocytes and tumor tissues confirmed the findings of WES (Figure 1C).

Sequencing of cDNA reverse-transcribed from RNA extracted from leukocytes revealed the heterozygous c.3046delA mutation and the wild-type A allele at the 5438 position. The cDNA sequence of the tumor tissues had predominantly the missense c.A5438T mutation (Figure 1C). The qRT-PCR revealed 54% of *DICER1* mRNA levels in the tumor tissues compared with those in the patient's leukocytes (Supplemental Figure 2). Pyrosequencing showed that cDNA of the proband's leukocytes consisted of 88% the wild-type allele and 12% the A-deletion allele, and all cDNA of the tumor tissues was the missense allele. The p.E1813V mutation affects a highly conserved amino acid residue within the ribonuclease (RNase) IIIb catalytic domain (Supplemental Figure 3) and is predicted to be damaging by both SIFT (Sorting Intolerant From Tolerant; http://sift.bii.a-star.edu.sg/www/SIFT_seq_submit2.html) and Polyphen2 (http://genetics.bwh.harvard.edu/pph2/) with scores of 0 and 1, respectively.

Discussion

Cushing's disease in infants and toddlers is very rare with only 14 cases (including the present case) reported to date (Table 1). In 2008, Scheithauer et al (10) first described a pituitary blastoma in a 13-month-old female with Cushing's disease,

Table 1. Summary of Reported Cases With Cushing's Disease in Infancy

Patient	Age, mo	Sex	Clinicals	Neuro-ophthalmopathy	Lab
1	8	M	Cushing's	Bitemporal hemianopia	HDDST: NS, ↑ ↑ ACTH
2	18	F	Cushing's	Ptosis	NA
3	11	M	Cushing's, cystic lungs and kidneys	Normal	↑ serum cortisol, ACTH– upper normal
4	18	F	Cushing's	Left ptosis, fixed pupils	HDDST:NS, pGHD
5	12	F	Cushing's, DI	NA	↑ ↑ plasma cortisol
6	7	F	Cushing's	Papilledema	↑ ACTH, ↑ cortisol
7	11	F	Cushing's, clitoromegaly	Visual inattention	↑ ACTH, ↑ cortisol
8	18	F	Cushing's	Normal	↑ ↑ pm cortisol
9	13	F	Cushing's, DI	NA	↑ Cortisol, ↑ ACTH
10	9	M	Cushing's, normal growth	Ophthalmoplegia, right ptosis	↑ Cortisol, ↑ ACTH
11	13	F	No Cushing's	Ophthalmoplegia, right ptosis	NA
12	24	F	No apparent Cushing's	Visual disturbance	↑ Cortisol, ↑ ACTH
13	9	M	Cushing's, FH of PPB, cystic nephroma, ovarian tumor	Right eye proptosis	Central hypothyroidism, ↑ AFP
14	12	F	Cushing's	Right ophthalmoplegia, right ptosis	↑ ACTH, ↑ cortisol HDDST-NS

Abbreviations: AFP, alpha-fetoprotein; CMT, chemotherapy; DI, diabetes insipidus; GT, gross total tumor removal; FH, family history; F, female; M, male; NA, not applicable; NS, nonsuppressible; pGHD, partial GH deficiency; postop, postoperative; PPB, pleuropulmonary blastoma; ST, subtotal tumor removal; XRT, radiotherapy.

in which pathology revealed a proliferation of ACTH-staining follicular cells at an early stage (~8–10 weeks gestation) of embryological differentiation. Early reports described these tumors as an unusual pituitary adenoma although some previous studies reported similar histologic description (1–4, 7, 9). Clinical experience with a pituitary blastoma is very limited. Most of these cases presented with Cushing's appearance, and neuro-ophthalmopathy. Although a small number of patients had evidence only of ACTH hypersecretion with clinically apparent Cushing's syndrome, most cases had pituitary macroadenoma. Notably, the low-dose dexamethasone suppression test and HDDST were mostly nonsuppressible. Although the HDDST is widely used to differentiate Cushing's disease from ectopic ACTH syndrome, its accuracy has been challenged in several adult and pediatric studies. Thus, this test is no longer recommended by a current guideline to test for Cushing's syndrome (16). The prognosis of infantile Cushing's was unfavorable with almost half of these children dying shortly after the diagnosis. Recent studies showed more favorable outcomes with polychemotherapy and adjuvant radiotherapy (9, 11).

A number of blastoma tumors, such as pleuropulmonary blastoma, cystic nephroma, ovarian Sertoli-Leydig cell tumor, embryonal rhabdomyosarcoma, and pineoblastoma are associated with germline *DICER1* mutations (15). A pituitary blastoma has been described in an infant with a family history suggestive of the *DICER1* syndrome, and a germline heterozygous *DICER1* mutation was identified in his leukocytes (12). No mutations in his tumor tissues were described. Here, we found novel germline and somatic *DICER1* mutations in a 1-year-old girl with a pituitary blastoma presenting with Cushing's disease. Therefore, pituitary blastoma is the expanded phenotype attributable to the *DICER1* cancer syndrome. Notably, previously reported cases with infantile Cushing's disease could be part of germline *DICER1* mutations.

The role of *DICER1* in normal pituitary development is not well-characterized. *Dicer1* knockdown in mice resulting in the loss of mature miRNA led to hypoplasia in the anterior pituitary, growth retardation, and decreased levels of GH, prolactin, and TSH (17). However, in this model, proopiomelanocortin expression was normal. The exact mechanism of germline *DICER1* mutations resulting in pituitary blastomas remains to be elucidated.

The effect of *DICER1* loss of function resulting in tumor development in humans will require further study. In nearly all cases where *DICER1* sequencing has been completed, the first inactivating hit was accompanied by a second hit in the RNase IIIb domain of *DICER1*, which is critical for miRNA interaction and cleavage, particularly at nucleotides encoding Asp1709 and Glu1813 (18). Previous studies demonstrated that these hot-spot somatic missense mutations did not obliterate DICER1 function but altered it in specific cell types (18–20). The authors suggested that aberrant miRNA processing from *DICER1* hot-spot mutations could be a key oncogenic event in this familial cancer syndrome.

Table 1. Continued

Tumor Size, cm	Histology	Treatment	Follow-Up	Ref.
12 × 8 × 5	Glandular structures within nests of pituitary adenoma cells, no mitotic activity	ST	Dead: postop 10 d	Miller et al, 1979 (1)
	Undifferentiated ACTH adenoma/ pleomorphism	ST 2/3 of tumor	Dead: postop due to pulmonary thromboembolism	Saeger et al, 1981 (2)
3	ACTH adenoma, a mixture of numerous follicles with sheet of tumor cells	GT twice	Alive	Sumner and Volbert, 1982 (3); Pullins et al, 1984 (4)
	Undifferentiated ACTH adenoma, 10% epithelial cells	ST 2/3 of tumor	Dead: intraoperative	Stegner et al, 1985 (5)
4 × 4 × 6, involved cavernous sinuses	Benign pituitary adenoma, $ACTH^+$	ST	NA	Maeder et al, 1996 (6)
2 × 2 × 3	Solid tissue with rosettes and tubular structures, $ACTH^+$ and TSH^+ ~5% of tumor cells	GT	Alive with remission at 1 y	List et al, 1999 (7)
3 × 2.5 × 2.5	NA	GT	Dead: immediate postop	Khadilkar et al, 2004 (8)
Large suprasellar mass	Follicular pattern with loss of acinar appearance and microcalcifications	GT	Alive with hypopituitarism	Moriarty and Hoe, 2009 (9)
3.5	Pituitary blastoma, rare mitoses	ST	Dead postop	Scheithauer et al, 2008 (10)
3 × 2.3 × 1.6, right cavernous sinus	Pituitary blastoma, high mitotic activity	ST + polyCMT	Alive with disease at 6 mo	Scheithauer et al, 2012 (11)
2.1 × 1.8, Rt cavernous sinus	Pituitary blastoma, high mitotic activity	ST + temozolomide + XRT	Alive with disease at 7 y	Scheithauer et al, 2012 (11)
4 cm, left cavernous	Pituitary blastoma, low mitotic activity	ST	Alive with panhypopituitarism at 5 y	Scheithauer 2012 (11)
1.6 × 3 × 2.3	Pituitary blastoma, brisk mitotic activity	ST + poly-CMT	Alive with stable disease at 22 mo	Wildi-Runge et al, 2011 (12)
2.9 × 2 × 2.8	Pituitary blastoma	ST + poly-CMT	Dead: postop 4 mo from complications of the catheter-port operation	This study

In our patient, her heterozygous germline mutation was insufficient to cause abnormal cell proliferation. It was only when a second somatic *DICER1* mutation occurred destroying DICER1's functions altogether that led to tumor initiation. From pyrosequencing of cDNA of the tumor tissues, we found that the germline frameshift allele was absent, suggesting that its mRNA was unstable, likely from nonsense-mediated mRNA decay. All detected *DICER1* sequence was from the somatic missense allele. It was in the RNase IIIb domain, agreeing with the previous knowledge that this domain was critical for DICER1's functions.

With the availability of next-generation sequencing, the extended phenotypes of the DICER1 syndrome will soon be more discovered. Endocrinologists should be aware of the possibility of *DICER1* mutations in various endocrine manifestations, such as Cushing's disease in infants, multinodular goiter in youth, and sex cord-stromal tumors, even in the context of a negative family history. Future studies investigating how inactivating *DICER1* has such specific effects may help understand a novel disease mechanism involved in miRNA perturbation and facilitate the development of more effective therapies for these patients.

Acknowledgments

Address all correspondence and requests for reprints to: Kanya Suphapeetiporn, MD, PhD, Division of Medical Genetics and Metabolism, Department of Pediatrics, SorKor Building 11th Floor, Faculty of Medicine, Chulalongkorn University, Bangkok 10330, Thailand. E-mail: kanya.su@chula.ac.th.

This study was supported by the Thailand Research Fund and Ratchadapiseksomphot Endowment Fund of Chulalongkorn University (RES560530177-HR).

Disclosure Summary: The authors have no conflict of interest.

References

1. **Miller WL, Townsend JJ, Grumbach MM, Kaplan SL.** An infant with Cushing's disease due to an adrenocorticotropin-producing pituitary adenoma. *J Clin Endocrinol Metab*. 1979;48:1017–1025.
2. **Saeger W, Ruttmann E, Lüdecke D.** ACTH secreting pituitary adenoma in an infant of 18 months. Immunohistochemical, electron-microscopic, and in-vitro studies. *Pathol Res Pract*. 1981;173:121–129.
3. **Sumner TE, Volberg FM.** Cushing's syndrome in infancy due to pituitary adenoma. *Pediatr Radiol*. 1982;12:81–83.
4. **Pullins DI, Challa VR, Marshall RB, Davis CH Jr.** ACTH-producing pituitary adenoma in an infant with cysts of the kidneys and lungs. *Histopathology* 1984;8:157–163.
5. **Stegner H, Lüdecke DK, Kadrnka-Lovrencic M, Stahnke N, Willig RP.** Cushing's disease due to an unusually large adenoma of the pituitary gland in infancy. *Eur J Pediatr*. 1985;143:221–223.
6. **Maeder P, Gudinchet F, Rillet B, Theintz G, Meuli R.** Cushing's disease due to a giant pituitary adenoma in early infancy: CT and MRI features. *Pediatr Radiol*. 1996;26:48–50.
7. **List JV, Sobottka S, Huebner A, et al.** Cushing's disease in a 7-month-old girl due to a tumor producing adrenocorticotropic hormone and thyreotropin-secreting hormone. *Pediatr Neurosurg*. 1999;31:7–11.
8. **Khadilkar VV, Khadilkar AV, Navrange JR.** Cushing's disease in an 11-month-old child. *Indian Pediatr*. 2004;41:274–276.
9. **Moriarty M, Hoe F.** Cushing disease in a toddler: not all obese children are just fat. *Curr Opin Pediatr*. 2009;21:548–552.
10. **Scheithauer BW, Kovacs K, Horvath E, et al.** Pituitary blastoma. *Acta Neuropathol*. 2008;116:657–666.
11. **Scheithauer BW, Horvath E, Abel TW, et al.** Pituitary blastoma: a unique embryonal tumor. *Pituitary*. 2012;15:365–373.
12. **Wildi-Runge S, Bahubeshi A, Carret A, et al.** New phenotype in the familial DICER1 tumor syndrome: pituitary blastoma presenting at age 9 months. *Endocr Rev*. 2011;32:P1–777.
13. **Chiosea S, Jelezcova E, Chandran U, et al.** Overexpression of Dicer

in precursor lesions of lung adenocarcinoma. *Cancer Res*. 2007;67:2345–2350.
14. **Hill DA, Ivanovich J, Priest JR, et al.** DICER1 mutations in familial pleuropulmonary blastoma. *Science*. 2009;325:965.
15. **Slade I, Bacchelli C, Davies H, et al.** DICER1 syndrome: clarifying the diagnosis, clinical features and management implications of a pleiotropic tumour predisposition syndrome. *J Med Genet*. 2011;48:273–278.
16. **Nieman LK, Biller BM, Findling JW, et al.** The diagnosis of Cushing's syndrome: an Endocrine Society Clinical Practice Guideline. *J Clin Endocrinol Metab*. 2008;93:1526–1540.
17. **Zhang Z, Florez S, Gutierrez-Hartmann A, Martin JF, Amendt BA.** MicroRNAs regulate pituitary development, and microRNA 26b specifically targets lymphoid enhancer factor 1 (Lef-1), which modulates pituitary transcription factor 1 (Pit-1) expression. *J Biol Chem*. 2010;285:34718–34728.
18. **Heravi-Moussavi A, Anglesio MS, Cheng SW, et al.** Recurrent somatic DICER1 mutations in nonepithelial ovarian cancers. *N Engl J Med*. 2012;366:234–242.
19. **Anglesio MS, Wang Y, Yang W, et al.** Cancer-associated somatic DICER1 hotspot mutations cause defective miRNA processing and reverse-strand expression bias to predominantly mature 3p strands through loss of 5p strand cleavage. *J Pathol*. 2013;229:400–409.
20. **Gurtan AM, Lu V, Bhutkar A, Sharp PA.** In vivo structure-function analysis of human Dicer reveals directional processing of precursor miRNAs. *RNA*. 2012;18:1116–1122.